BIOPHYSICAL PROPERTIES OF CROSSLINKED POLY (PROPYLENE FUMARATE)/HYDROXYAPATITE NANOCOMPOSITES

NAGWA A. KAMEL, SALWA L. ABD-EL-MESSIEH*, SAMIA H. MANSOUR**, BERLENTY A. ISKANDER***, WAFAA A. KHALIL****, K.N. ABD-EL-NOUR*

*Microwave Physics and Dielectrics Department, National Research Centre, Dokki, Cairo, Egypt,
#corresponding author: e-mail: abdelnourkn@yahoo.com
**Polymers and Pigments Department, National Research Centre, Dokki, Cairo, Egypt
***Engineering Department, American University, Cairo, Egypt
****Biophysics Department, Faculty of Science, Cairo University, Egypt

Abstract. Polypropylene fumarate (PPF) as unsaturated polyester was prepared to be crosslinked with three different monomers, namely N-vinyl pyrrolidone (NVP), methyl methacrylate (MMA) and a mixture of NVP and MMA (1:1 weight ratio) and were filled with different concentrations of hydroxyapatite (HA) 40, 45 and 50 wt%. The bone apatite which is expected to be formed on the surface of the samples after immersion in simulated body fluid (SBF) has been studied through different tools. Fourier transform infrared (FTIR) used for characterizing the composites through the band assignments of different groups. The results of scanning electron microscope (SEM) and energy dispersive X-ray (EDX) confirmed the layer formed on the surface through the SEM images and phosphocalcic ratios. The dielectric relaxation mechanisms which were studied at frequency range from 102 to 105 Hz through Fröhlich and Havriliak-Negami functions is considered to be a good support to the formation of such a layer on the surface of the composite. The degradation rate and degradation mechanism are also taken into consideration.

Key words: poly (propylene fumarate), hydroxyapatite, nanocomposites crosslinking agent, biodegradable, biophysical properties.

INTRODUCTION

In recent years, there has been a marked increased interest in biodegradable materials for use in packaging, agriculture, medicine, and other areas [25].

The mixing of bioactive nanoparticles with polymers to form composite materials open new research pathways for introducing new composites that exhibit advantages in the biomaterial field [40].

Received: January 2013;
in final form April 2013

ROMANIAN J. BIOPHYS., Vol. 22, Nos 3–4, P. 189–214, BUCHAREST, 2012

Polypropylene fumarate (PPF) is an amorphous polymer with a glass transition temperature (T_g) varying with molecular weight up to 31°C. The biocompatible and extractable degradation products, primarily fumaric acid and propylene glycol, upon hydrolysis of its ester linkages made it a promising candidate to be used in the biomaterial field [10]. The propylene glycol part in each repeating unit of PPF chain provides only one free rotating carbon-carbon single bond. This rigidity of PPF polymer chain limits the accessibility of double bonds during polymerizing and ester bonds during degradation. Due to this rigidity, a crosslinker molecule is often required to crosslink PPF [43]. The choice of the crosslinker that will create the links between PPF chains is very important; it has to be biocompatible and also compatible with PPF [13].

Several crosslinking agents were used such as methylmethacrylate (MMA), N-vinyl pyrrolidinone (NVP) and biodegradable macromers of PPF-diacrylate or poly (ethylene glycol)-diacrylate [15]. Our previous work investigated the use of NVP, MMA and a mixture of them as crosslinking agents for PPF and calcium sulphate dihydrate (Gypsum) as filler. The dielectric, mechanical and biological properties of PPF composites were studied [20].

The use of a bioactive filler such as hydroxyapatite (HA), ceramic or bioglass particles to reinforce a polymer may improve both the mechanical properties and the bone bonding properties [26]. Hydroxyapatite [$Ca_{10}(PO4)_6(OH)_2$] is not only a biocompatible, osteoconductive, non toxic, non inflammatory and non immunogenic agent, but also bioactive, it has got the ability to form direct chemical bonds with living tissues [9, 35].

Jayabalan *et al*. [19] studied the effect of hydroxyapatite on the performance of nanocomposites of hydroxy-terminated high molecular weight poly(proplyene fumarate) (HT-PPFhm), They concluded that calcined HA nanoparticles resulted in very good crosslinking in the resin matrix with high crosslinking density and interfacial bonding with the polymer, owing to the rod-like shape of the nanoparticles, this gave improved biomechanical strength and modulus and also controlled degradation of the nanocomposite for scaffold formation.

Deep insight into the interaction between electric fields and molecules has resulted in many new applications. One of these nontraditional applications is to follow up the degradation of the biodegradable polymers composites using the dielectric spectroscopy [16].

Surface properties have an enormous effect on the success or failure of a biomaterial. Microscopy techniques including scanning electron microscopy (SEM), transmission electron microscopy (TEM) are proving useful in the analysis of the surface properties of polymeric biomaterials. In addition to imaging the surface morphology of polymeric biomaterials, the SEM can be combined with other analysis methods such as energy dispersive X-ray analysis (EDX) to determine elemental distribution and IR and Raman spectroscopy to monitor surface modification procedures. EDX results are typically obtained from a

sampling depth of the order of micrometers, thus are more representative for the bulk material rather than the surface [29].

A series of polyurethane\nano-hydroxyapatites with different hydroxyapatite content was studied by Martinez-Valencia *et al*. [27]. Characterization, bioactivity, and biodegradability of these materials were done using XRD, FTIR, and SEM-EDX techniques.

The combination of gelatin with a bioactive hydroxyapatite and cartilage powder was studied to form biocomposites that can be applied as bone implants. The resulting biocomposites were assessed by ATR-IR and SEM-EDX techniques to prove the interaction between different matrices [12].

The objective of the present work is to develop new composites based on polypropylene fumarate crosslinked with N-vinylpyrrolidone, methylmethacrylate and a mixture of them (1:1 wt%) loaded with different concentrations of hydroxyapatite to be used as bone implants. The apatite layer which is expected to be formed onto the surface of the samples by immersion in simulated body fluid (SBF) will be studied through the dielectric measurements, Fourier transform infrared (FTIR), scanning electron microscope (SEM), energy dispersive X-ray (EDX). The biodegradation mechanism involving the change in pH and weight loss during immersion in simulated body fluid (SBF) will be also taken into consideration.

EXPERIMENTAL WORK

MATERIALS

Diethyl fumarate, 1, 2-propanediol, and tetrabutyl titanate as the transesterification catalyst were reagent grade from Merck, Darmstadt, Germany, and used as received. N-vinyl pyrrolidone (NVP; freshly distilled) or methyl methacrylate (MMA; freshly distilled) were obtained from Merck, Darmstadt, Germany. Benzoyl peroxide, N, N-dimethyl-4-toluidine and hydroxyapatite were obtained from Sigma-Aldrich (Germany).

Preparation of Polypropylene fumarate (PPF) carried out by the two-stage melt polycondensation method (esterification and polycondensation) and crosslinked with 30% by weight of (N-vinyl pyrrolidone (NVP), methylmethacrylate and a mixture of (NVP and MMA) in the ratio of (1:1) by weight. An extensive description of the preparation and characterization of PPF can be found elsewhere [20].

The composites were prepared by mixing different ratios of hydroxyapatite (40, 45 and 50 wt%) with a mixture of fumarate polyester resin and crosslinking agents, namely NVP, MMA, and a mixture of NVP and MMA (1:1 wt%) (NVP/MMA). The samples were left for 24 h at 25 °C for curing.

In order to detect the bioactivity, the composites were immersed in simulated body fluid (SBF) solution. The solution was prepared according to Kokubo *et al*. [23] by dissolving appropriate amounts of NaCl, $NaHCO_3$, KCl, $K_2HPO_4{\cdot}3H_2O$, $MgCl_2{\cdot}6H_2O$, $CaCl_2$ and Na_2SO_4 in distilled water and buffering to pH 7.4 at 36.5 ^oC with tris (hydroxymethyl)amino methane and 1 M HCl solution. After 30 days, the samples were removed, rinsed with distilled water and then dried at room temperature.

Degradation experiments for the composites were conducted by immersing the specimens in SBF solution of pH 7.4 at 36.5 ^oC. Weight changes were monitored after predetermined time periods by removing the samples from the solution and wiping the excess liquid. Weight changes were calculated at each time period as follows:

$$\%weight\_loss = \frac{W_t - W_0}{W_0} \times 100 \quad (1)$$

W_t and W_0, are weights of the wet and starting dry discs at time t.

The pH changing during immersion in SBF was carried out using pH meter (PCSIR manufactured).

TECHNIQUES

Transmission electron microscope was used to determine the particle size of the fillers using model: Tecnai G 20, Super twin, double tilt and Magnification range up to 1,000,000 x and applied voltage 200 kV. Gun type: LaB_6Gun, Japan.

Scanning electron microscope coupled with energy dispersive X-ray (SEM/EDX, Philips XL30) Japan was used to study the morphology of the composite before and after soaking in SBF.

Fourier transform infrared (FTIR) was used to record the infrared spectrum by using JASCO FT/IR 300 E (Tokyo, Japan)**.**

Dielectric measurements were carried out in the frequency range 100 Hz up to100 kHz using (Ando Electric, Japan). The capacitance C, loss tangent tan δ, and ac resistance R_{ac} were measured directly from the bridge from which the permittivity ε', dielectric loss ε" and R_{dc} were determined. A guard ring capacitor type NFM/5T Wiss Tech. Werkstatten (WTW) GMBH Germany was used as a measuring cell. The cell was calibrated using standard materials and the experimental errors in ε' and ε" were found to be ±3% and ±5%, respectively. The temperature was controlled to 30 ^oC by using digital oven and the experimental error in the temperature was ±0.1 °C.

The compressive tests were conducted according to ASTM D 695-ISO 604. The cylindrical specimens were prepared for compression test with aspect ratio 2:1 (length to diameter ratio). Hounsfield (100 KN) universal testing machine was used. Axial compressive load was applied to the specimen with head speed 3 mm/min.

RESULTS AND DISCUSSION

MICROSCOPIC CHARACTERIZATION

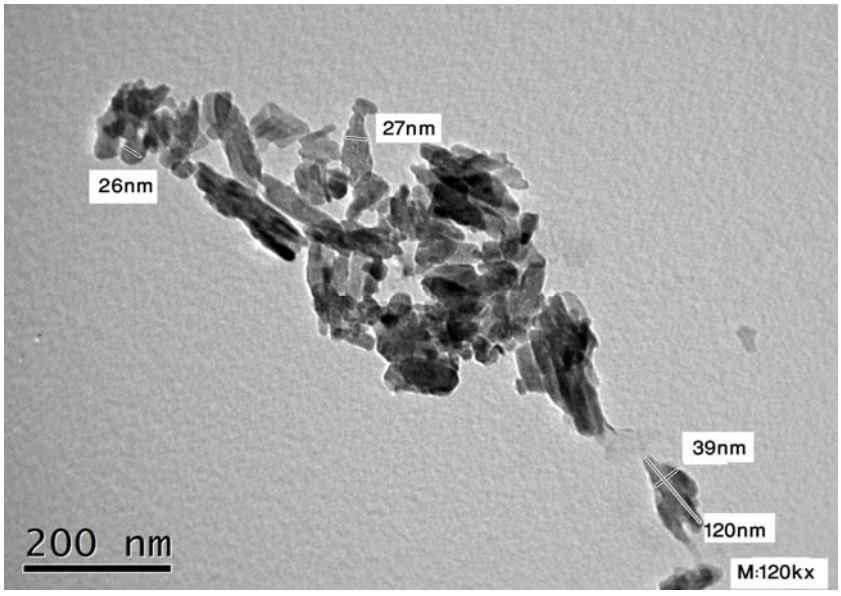

Fig. 1. TEM micrograph of the hydroxyapatite particles.

Figure 1 illustrates the TEM micrograph of the hydroxyapatite particles used in this study. The image shows that the sample exhibits needle-like morphology. The particle size was found to be in the range of 26–120 nm. This result is in good agreement with the HA micrographs previously observed by Chen *et al*. [5].

FTIR CHARACTERIZATION

FTIR spectra of polypropylene fumarate (PPF), hydroxyapatite (HA) are recorded in the spectral region 4000–400 cm^{-1} and represented in Figure 2. The band assignments are given in Tables 1 and 2, respectively.

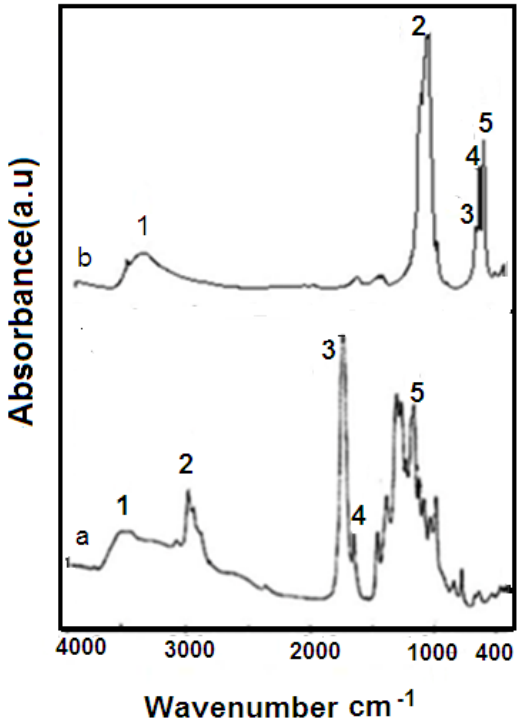

Fig. 2. FTIR spectra of (a) polypropylene fumarate (PPF) and (b) hydroxyapatite (HA).

Table 1

FTIR band assignments for PPF [20]

Band No.	**Bands (cm^{-1})**	**Assignments**
1	3446	OH groups
2	2960	stretching frequency of CH_2
3	1730	stretching frequency of acid and ester carbonyl group
4	1643	unsaturation C=C in fumarate unit
5	1000–1300	C–O stretching vibrations

Table 2

FTIR band assignments for HA [8]

Band No.	**Bands (cm^{-1})**	**Assignments**
1	3555	stretching mode of hydrogen-bonded OH^- ions
2	1031	Stretching mode of PO_4^{-3}
3	622	liberational mode of hydrogen bonded OH^- ions
4	603	Bending mode of PO_4^{-3}
5	561	Bending mode of PO_4^{-3}

The FTIR spectra for PPF\HA composites are gathering all the characteristic bands of the polymer and the hydroxyapatite. The spectra were investigated before and after immersion in SBF for 30 days and represented in Figure 3. The composites crosslinked with NVP/MMA were chosen as an example.

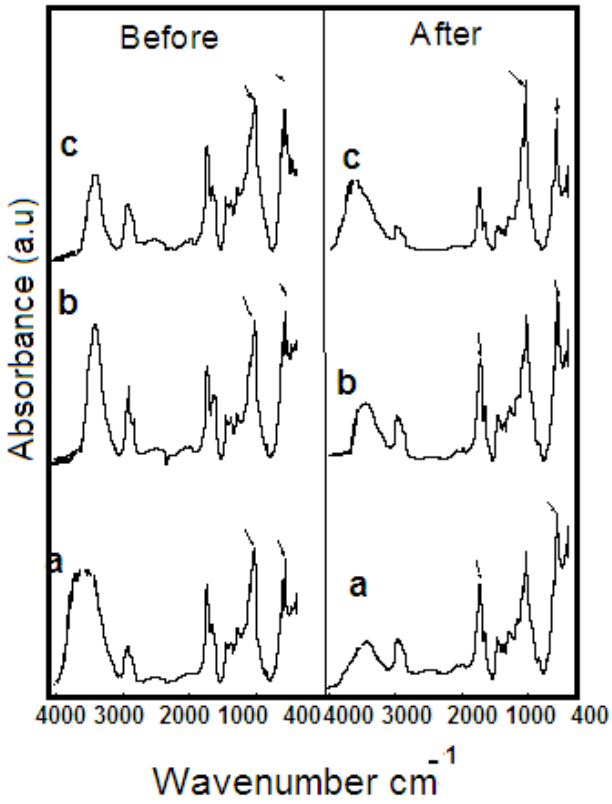

Fig. 3. FTIR spectra of PPF\HA composites crosslinked with NVP\MMA and filled with different concentrations of HA (a) 40% (b) 45% (c) 50wt% before and after immersion in SBF for 30 days.

Before immersion, there is a significant increase in the intensities of the 1030 and 566 cm^{-1} bands characteristic for the phosphate group by increasing the HA content [22]. It is important to state that the same behavior is observed for the MMA, NVP crosslinked composites. There is similarity between pre and post immersion in SBF and this is the expected result when the bioactive layer formed is similar to the filler in the composites. The changing character of the bands, the change of their intensity and width at half height are connected with the process of hydrolysis of the polymer and the breaking of the bonds in the chain [6].

For the polymer the band with 1737 cm^{-1} characteristic of the stretching frequency of acid and ester carbonyl group possesses the highest intensity; it was selected as the reference point in the analysis of the relations with the remaining

bands. For the HA filler the intensity of the 566cm^{-1} characteristic of the vibration of the phosphate group was chosen for comparing the intensity before and after immersion in SBF the results being displayed in Figures 4 and 5).

The intensity of the peaks related to the wave number 1737cm^{-1} characteristic for the polymer decreases after immersion as a result of the degradation occurred in the polymer matrix. While the band at 566cm^{-1} which is characteristic for the HA is found to increase after immersion of the samples in SBF. This is a good evidence for the formation of bone apatite layer onto the surface of the investigated samples.

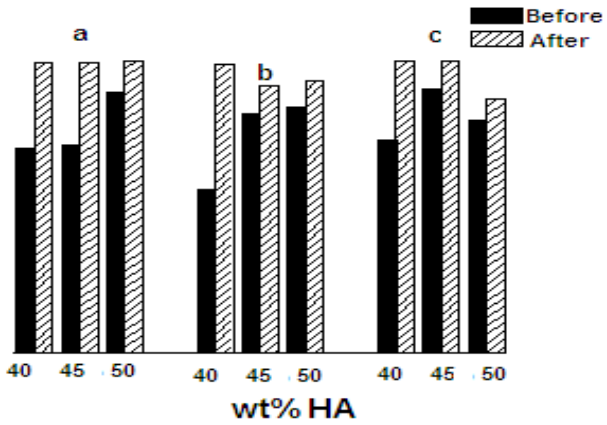

Fig. 4. Intensities of 566 cm^{-1} band for PPF\HA samples crosslinked with MMA, (b) NVP, (c) NVP\MMA before and after immersion in SBF for 30 days.

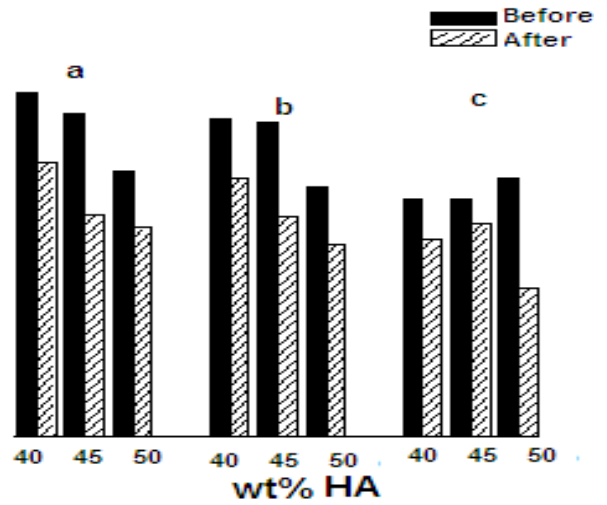

Fig. 5. Intensities of 1737 cm^{-1} band for PPF\HA samples crosslinked with (a) MMA, (b) NVP (c) NVP\MMA before and after immersion in SBF for 30 days.

EVALUATION OF THE BIOACTIVITY OF COMPOSITES

SCANNING ELECTRON MICROSCOPE (SEM) AND ENERGY DISPERSIVE X-RAY (EDX) ANALYSIS

The bioactivity is defined as the ability of the material to make interfacial bonding with the surrounding tissues [7]. This bioactivity is laboratory evaluated by means of the formation of a biologically active hydroxyapatite layer on the implant surface after immersion in SBF solution [24]. To test the bioactivity in our study, surface morphology of the crosslinked PPF/HA 45 wt% disks was examined by a scanning electron microscope (SEM) and the elemental analysis carried out by energy dispersive X-ray (EDX) technique before and after 30 days of immersion in SBF. The data are represented in Figure 6 for sample PPF/HA crosslinked with NVP/MMA and filled with 45 wt HA as an example.

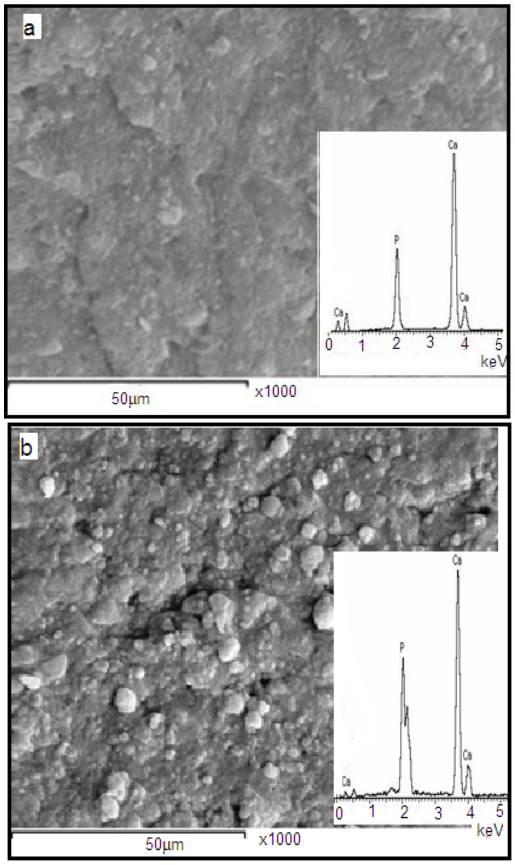

Fig. 6. SEM micrograph and EDX spectrum of PPF/HA samples crosslinked with NVP/MMA and filled with 45 wt% HA (a and b) before, (c and d) after immersion in SBF for 30 days.

Before immersion in SBF, the SEM micrographs (Figure 6a) show a smooth surface which revealed a homogeneous distribution of the HA particles within the polymer matrix. During immersion in SBF surface roughness could be observed. The roughness increases with increasing the immersion time. The surface began to exhibit surface pores due to the degradation of the polymer. The degradation of the polymer results in more exposure of the bioactive HA filler to the SBF leading to nucleation of the bioactive calcium phosphate layer by consuming the calcium and phosphorus ions from the solution.

After 30 days of immersion (Figure 6b), the surfaces were analyzed by scanning electron microscope. The bioactivity of the composites was confirmed by the presence of small and large spherical particles with bright color denoting deposition of calcium phosphate particles which coated all the surface.

From the EDX profile the main chemical elements of the PPF\HA composites before immersion were identified as carbon (C) and oxygen (O_2) originating from the PPF polymer structure, calcium (Ca) and phosphorus (P) originating from the incorporated HA, After 30 days of immersion in SBF the EDX analysis revealed the presence of the same elements and the spectrum showed an increase in both calcium and phosphorus signals as a result of the growth of HA. Table 3 shows the concentrations of calcium and phosphorus elements of the PPF/HA composites before and after immersion in SBF using EDX technique. The Ca-P ratios of the samples after immersion for 30 days in SBF are 1.58, 2.03 and 1.66 for PPF/HA composites crosslinked with MMA, NVP and NVP/MMA respectively which are very close to the stoichiometric biological apatite (1.67) [30]. The increased phosphocalcic ratio for NVP crosslinked PPF\HA samples may attribute to the presence of negatively charged carboxylate group of N-vinylpyrrolidone which may attract calcium ions present in the SBF solution and favor calcium phosphate apatite nucleation.

Table 3

Calcium and phosphorus concentrations for the PPF\HA composites crosslinked with MMA, NVP\MMA and NVP before and after immersion in SBF for 30 days

Element	Concentrations of elements (at. %)	
	Before immersion	After immersion
PPF/HA crosslinked with MMA		
Phosphorus	8.20	9.17
Calcium	14.24	14.53
Molar Ca/p ratio	1.74	1.58
PPF/HA crosslinked with NVP/MMA		
Phosphorus	3.2	11,11
Calcium	5.16	18.39
Molar Ca/p ratio	1.61	1.66
PPF/HA crosslinked with NVP		
Phosphorus	7.27	12.87
Calcium	14.68	26.16
Molar Ca/p ratio	2.02	2.03

The results of the SEM and EDX are complementary and confirmed that the layers formed on the surfaces of the composites are bone like apatite according to their SEM images and phosphorcalcic ratio.

BIODEGRADABILITY TEST

Degradation of PPF as an aliphatic polyester undergoes bulk degradation, where material is lost from the entire polymer volume at the same time due to water penetrating the bulk. So the rate of degradation of these polymers depends on the extent of water accessibility to the matrix rather than the intrinsic rate of ester cleavage. The water accessibility to the matrix depends on several factors such as the hydrophobicity /hydrophilicity of the polymer, the crystallinity of the polymer, and the dimension of the sample [34]. The weight loss of the PPF\HA samples crosslinked with NVP/MMA filled with 45 wt% HA as an example is represented in Figure 7.

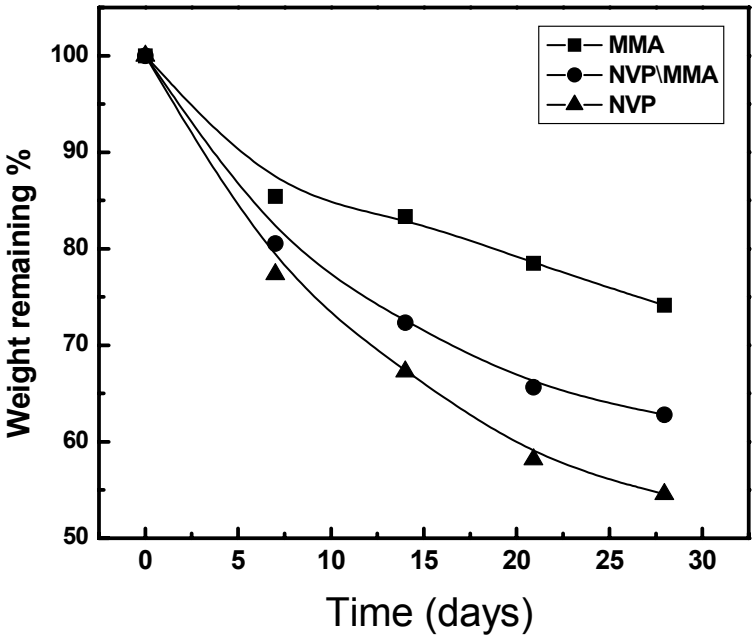

Fig. 7. Degradation rate of PPF\HA composites crosslinked with NVP, MMA and NVP/MMA and filled with 45%wt HA *versus* time (days).

From Figure 7 it is seen that the degradation rate of the samples follows the order NVP > NVP\MMA > MMA. Same trend was observed for all concentrations. It is worth mentioning that the degradation rate decreases with increasing the HA

content in the order 40 > 45 > 50wt%. In Figure 8, HA is partially neutralizing the biodegradable product acids of the polymer. These acid products can act as catalyst and accelerate the hydrolysis reaction. The hydroxyl groups in HA react with the acids leading to inhibit the acid catalysis which in turn reduces the biodegradation rate [11].

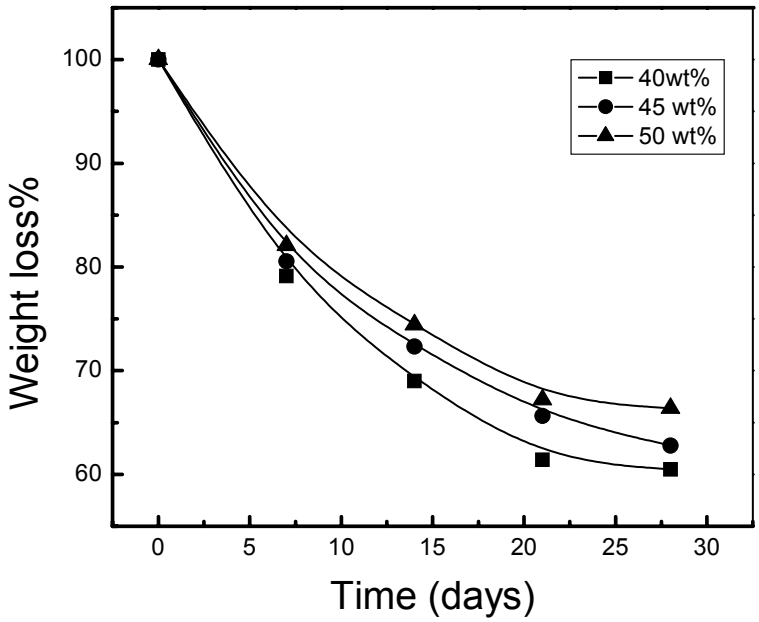

Fig. 8. Degradation rate of PPF\HA composites crosslinked with NVP\MMA and filled with 40, 45 and 50 wt% HA *versus* time (days).

pH CHANGING DURING IMMERSION

The pH of the SBF solution during immersion of the samples is measured to monitor the changes that could be a combination of acidic degradation byproducts resulting from the polymer and any neutralization effects resulting from the filler.

The changes of the pH values of SBF for PPF\HA composites filled with 45 wt% with different crosslinking agents are shown in Figure 9.

For all samples there was a rapid decrease in the pH of the SBF at the first 3 days of immersion as a result of dissolution of the composites which suggest high reactivity of these composites. The decrease in the pH values reached the lowest value ranging from 4–4.5 at the end of the immersion time.

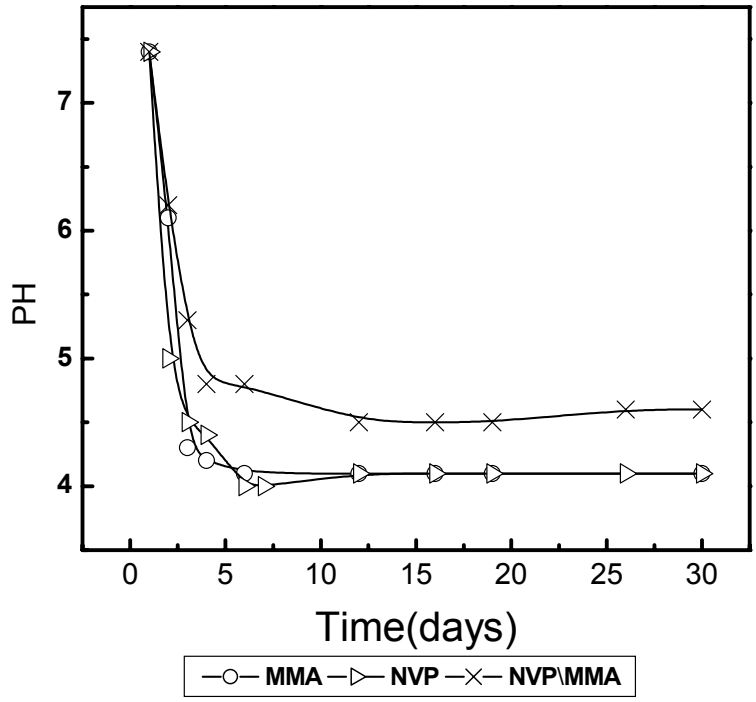

Fig. 9. The change in the pH values of the SBF during immersion of PPF\HA samples filled with 45 wt% HA.

DIELECTRIC STUDIES

The frequency dependence of the permittivity ε' and dielectric loss ε" over the frequency range from 100 Hz – 100 KHz and at 30°C for polypropylene fumarate (PPF) crosslinked with different crosslinking agents (NVP, MMA, NVP/MMA and their composites filled with different concentrations of HA (40, 45 and 50 wt%) are illustrated graphically in Figure 10.

From this figure it can be seen that ε' for all investigated samples decreases with increasing the frequency, which shows anomalous dispersion. On the other hand, the absorption curves of ε" *versus* the frequency *f* shown in Figure 10 are broad indicating that more than one relaxation mechanism is present. It is also clear that the values of ε' and ε" increase in the order MMA < NVP/MMA< NVP. This may be due to the higher polarity of NVP (4.0 D) [18] compared with that of MMA, (1.79 D) [1]. From this figure it is seen that the values of ε' and ε" are higher at a lower frequency range, but at higher frequencies both became relatively constant. A similar behavior was observed in a number of polymers [21, 32, 38]. Such high values of ε' may be due to the interfacial effects within the bulk of the

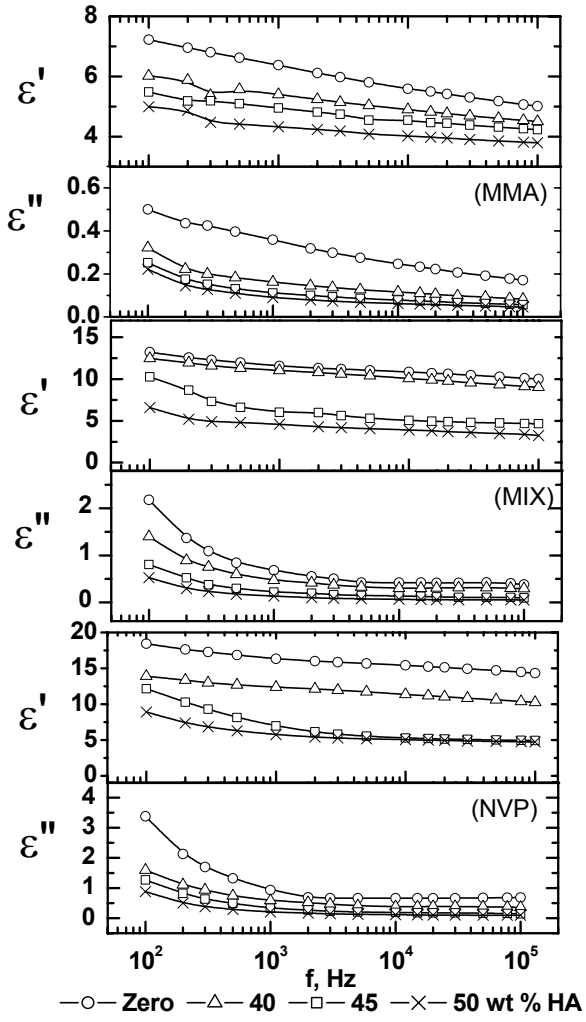

Fig. 10. The permittivity ε' and dielectric loss ε“ *versus* frequency f of PPF\HA composites crosslinked with MMA, NVP and NVP/MMA and filled with different concentrations of HA (40, 45 and 50 wt%).

sample and the electrode effects and/or Maxwell Wagner polarization [37, 39]. The values of both ε' and ε" are found to be comparable with those found before in literature [20]. When an electric field is applied to the materials, the long-range drift of ions and barrier layer formation on the electrode surface result in large values of permittivity and dielectric loss [33, 36]. At high frequencies, the periodic reversal of the electric field occurs so fast that there is no excess ion diffusion in the direction of the field. The polarization due to the charge accumulation decreases, leading to a decrease in the values of ε' and ε" [4, 42]. On the other

hand, the absorption curves of ε" *versus* the frequency *f* shown in Figure 10 are broad indicating that, in addition to the electrical conductivity, more than one relaxation mechanism is present [3]. After subtracting the conductivity term, the analysis of the absorption curves was done in terms of superposition of Fröhlich function distribution parameter $p = 3$ and a Havriliak-Negami function with distribution parameter $\alpha = 0.5$ and $\beta = 0.5$ according to the equations given elsewhere [2]. The obtained data are given in Table 4.

Table 4

Relaxation parameters using Fröhlich (1) and Havriliak-Negami (2) functions for PPF\HA composites crosslinked with NVP, MMA and NVP/MMA filled with 40, 45 and 50% HA

HA content (%)	τ_1 (s)	S_1	$\tau_2 \times 10^{-5}$ (s)	S_2	$\sigma \times 10^{-11}$ (s/m)
PPF/HA crosslinked with MMA					
0			3.33	1.29	1.6
40	0.0003	0.214	3.5	0.607	1.3
45	0.0003	0.144	3.79	0.409	1.1
50	0.0003	0.112	4.20	0.336	1.0
PPF/HA crosslinked with NVP					
0			0.74	4.32	19.5
40	0.0003	2.26	1.509	1.595	10.3
45	0.0003	0.362	1.803	0.986	7.4
50	0.0003	0.195	2.2	0.622	4.4
PPF/HA crosslinked with NVP/MMA					
0	0.0004	0.616	1.5	2.50	13
40	0.0003	0.57	1.8	1.85	6.7
45	0.0003	0.28	2.1	0.722	3.9
50	0.0003	0.138	2.7	0.337	2.6

An example of the analyses is given in Figure 11 for PPF crosslinked with the three different monomers and loaded with 45 wt% HA.

This Figure indicates that an absorption region is detected at lower frequency range which is fitted by Fröhlich function [17] with distribution parameter $p = 3$ and relaxation time ranging $3–4 \times 10^{-4}$ s. The relaxation time associated with such process is found to be independent of the type of monomer used for crosslinking. This absorption region could be attributed to Maxwell-Wagner effect [17] as it is expected to be at the lower frequency range due to the multi-constituents of the investigated systems [20].

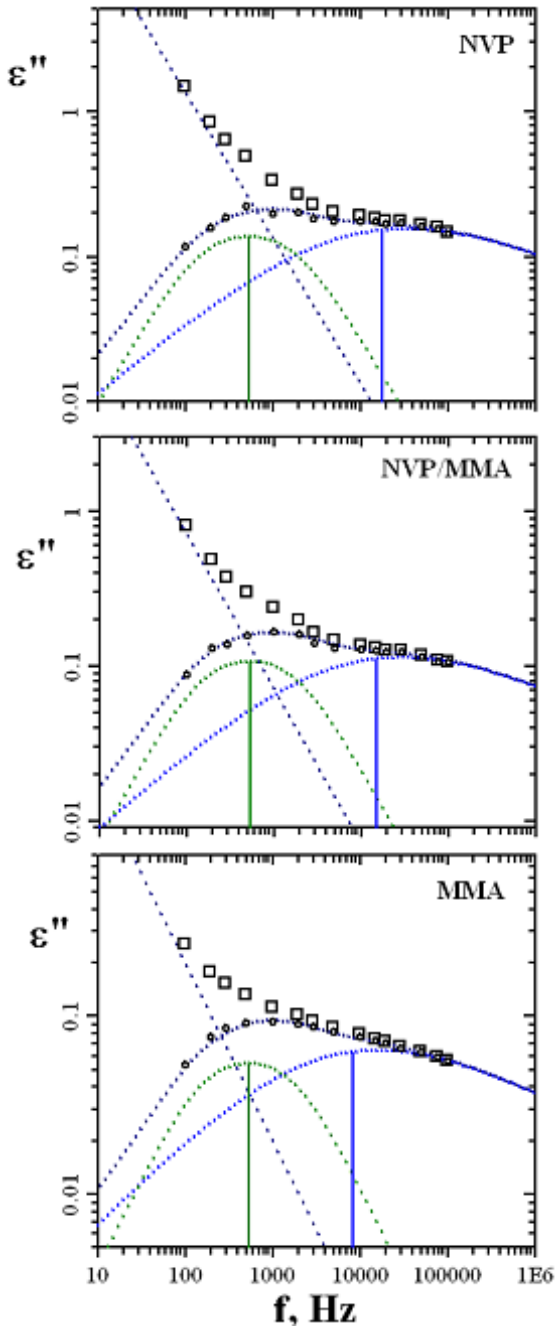

Fig. 11. Example of the analysis for PPF\HA composites crosslinked with MMA, NVP and NVP/MMA loaded with 45 wt% HA. The data are fitted by Fröhlich Function and Havriliak-Negami functions in addition to the conductivity term.

The second absorption region in the higher frequency range could be associated with some local molecular motions rather than with the main chain motion as it is expected to be frozen because the measurements were carried out at 30 ^{o}C, i.e. lower than the glass transition T_g of the crosslinked polyester [28]. This relaxation corresponds to the terminal polar groups, carboxyl and hydroxyl functions, and to ester functions in the polymer chain [14]. The relaxation time associated with this region is found to be highly affected by the type of crosslinking agent and follows the order MMA > NVP/MMA > NVP, i.e. depending on the molar volume of the rotating units and consequently on the relaxation time [20].

From Table 4, it is notable that by increasing the filler content the values of the relaxation time τ_2 increase while the electrical conductivity σ and the relaxation strength S_2 decrease.

On the other hand, from this table it is deduced that the previous properties τ_2, σ and S_2 for the samples crosslinked with NVP and NVP/MMA are not linearly fitted. This non-linearity, which is noticed throughout the whole-investigated systems containing the different percentages of HA, exhibits an additional molecular order in case of crosslinked sample with NVP/MMA. This deviation could be attributed to some sort of molecular interaction between MMA and NVP which is expected to take place. This proposed interaction could lead to an increase in the molar volume and consequently the relaxation time [1]. This result finds further justification through the conductivity measurements as well as the relaxation strength.

After immersing the crosslinked samples without filler and those containing different concentrations of HA in SBF solution for four weeks, the permittivity ε' and dielectric loss ε'' were re-measured (Figure 12).

Comparing the data obtained before and after immersing in SBF (Figures 10 and 12) it is seen that both ε' and ε'' decrease by immersing in the SBF solution. This decrease could be due to the formation of apatite structure that takes some ions to crystal formation where they are no longer mobile and no longer contributing to the dielectric spectrum [31]. The curves relating ε'' and the applied frequency f were analyzed into two absorption regions. The first region was found to be unchanged and could ascribe Maxwell Wagner effect. The second region ascribes the local molecular motions. The analyses given for polypropylene fumarate crosslinked with NVP and loaded with 45 wt% HA before and after immersing in SBF solutions are illustrated graphically in Figure 13. The data obtained from the analyses are listed in Table 5.

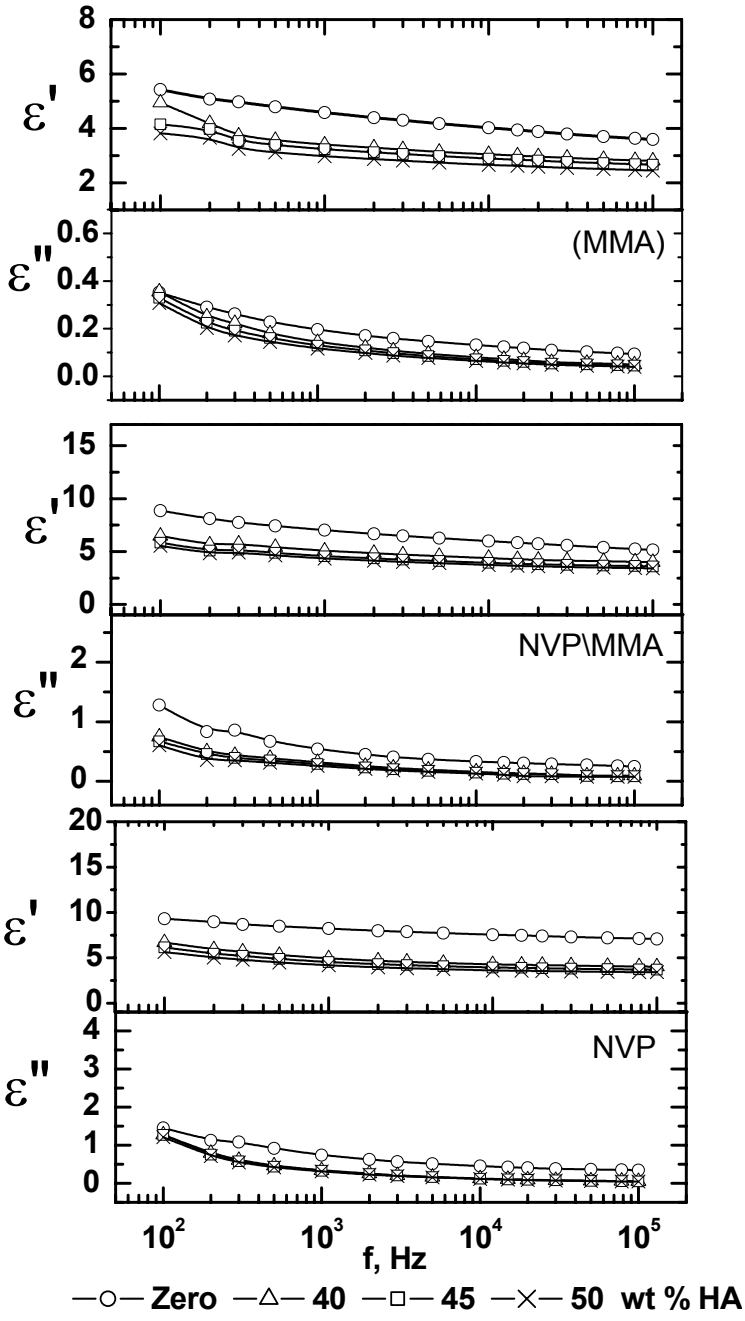

Fig. 12. The permittivity ε' and dielectric loss ε'' *versus* frequency *f* of PPF\HA composites crosslinked with MMA, NVP and NVP / MMA, filled with different concentrations of HA (40, 45 and 50 wt%) after immersion in SBF for 30 days.

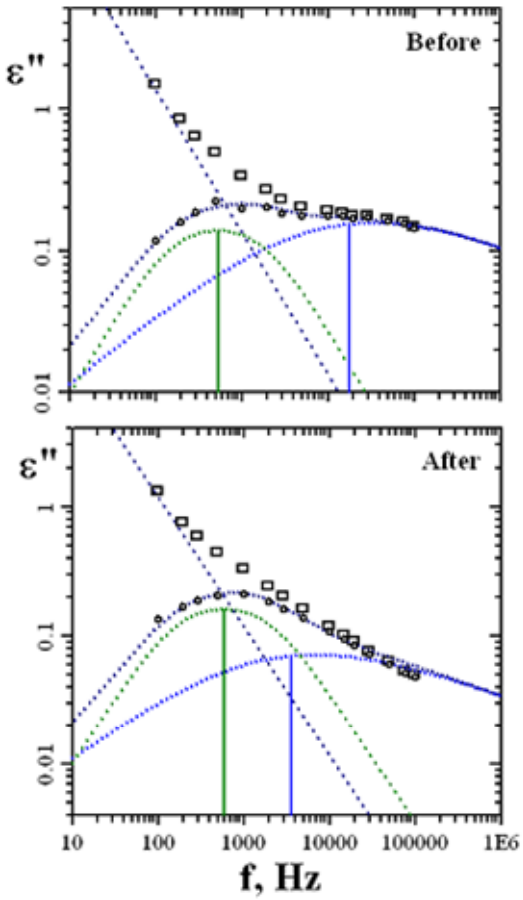

Fig. 13. Example of the analysis for PPF/HA composites crosslinked with NVP and loaded with 45 wt% HA before and after immersion in SBF for 30 days. The data are fitted by using Fröhlich and Havriliak-Negami function in addition to the conductivity term.

Table 5

Relaxation parameters using Fröhlich (1) and Havriliak-Negami (2) functions for PPF\HA composites crosslinked with MMA, NVP and NVP/MMA loaded with 40, 45 and 50 wt% HA after immersion in SBF for 30 days

HA content (%)	τ_1 **(s)**	S_1	$\tau_2\times10^{-5}$ **(s)**	S_2	$\sigma\times10^{-11}$ **(s/m)**	$(\tau_{aft}-\tau_{bef})/\tau_{bef}$
PPF\HA crosslinked with MMA						
0	0.0004	–	6.20	0.72	1.4	0.862
40	0.0004	0.216	7.64	0.402	1.4	1.18
45	0.0004	0.355	11.00	0.198	1.4	1.90
50	0.00035	0.3155	11.79	0.3155	1.3	1.81

Table 5 (continued)

PPF/HA crosslinked with NVP/MMA						
0	–	–	5.02	1.87	6.7	1.89
40	0.0003	0.487	6.5	0.7	3.3	2.6
45	0.0003	0.44	8.8	0.637	3.0	3.19
50	0.00036	0.40	9.03	0.611	2.6	2.33
PPF/HA crosslinked with NVP						
0	–	–	2.9	2.35	6.5	2.93
40	0.0003	0.473	6.91	0.434	6.5	3.6
45	0.00028	0.394	8.73	0.394	6.5	3.85
50	0.00025	0.384	9.33	0.385	6.3	3.24

Comparing Tables 4 and 5 it is interesting to find that both conductivity and S_2 decrease while a pronouncing increase in τ_2 is noticed. The increase in τ_2 reflects an increase in the molar volume of the rotating units due to the formation of apatite structure that takes some ions to crystal formation to become no longer mobile and thus no longer contributing to dielectric spectrum.

In order to find an expression to distinguish between the amounts of apatite structure which is assumed to be formed by immersing the investigated samples in SBF, the relation $(\tau_{aft} - \tau_{bef})/\tau_{bef}$ was calculated and listed in Table 5. From this table it is interesting to notice that the values of $(\tau_{aft} - \tau_{bef})/\tau_{bef}$ increase by the addition HA up till 45% HA after which a slight decrease was noticed at concentration 50%. This increase was found to follow the order NVP > NVP/MMA > MMA. This finding is found to be comparable with that found before in case of PPF/gypsum composites [20]. Figure 14 represents the variation of $(\tau_{aft} - \tau_{bef})/\tau_{bef}$ *versus* NVP content for samples containing 40 and 45 wt% HA.

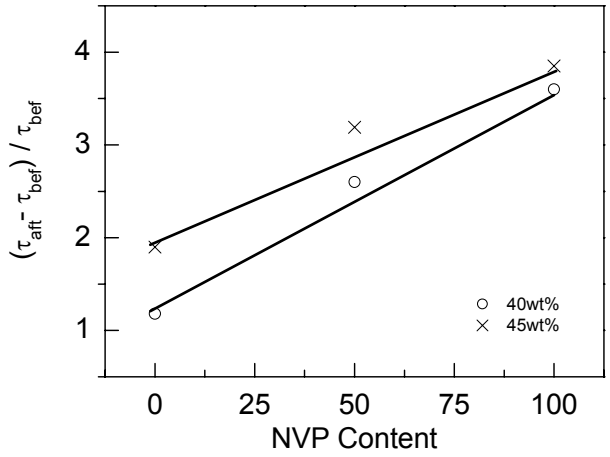

Fig. 14. The variation of $(\tau_{aft} - \tau_{bef})/\tau_{bef}$ *versus* NVP content for samples containing 40 and 45 wt% HA.

This figure indicates that the values of $(\tau_{aft} - \tau_{bef})/\tau_{bef}$ for NVP/MMA deviates positively from the line connecting the two individuals. This positive deviation indicates that the properties of polypropylene fumarate crosslinked with NVP/MMA are shifted towards those crosslinked with NVP rather than MMA. These results could recommend the NVP/MMA to be used in crosslinking polypropylene fumarate rather than the expensive monomer NVP and the unrecompensed one MMA.

MECHANICAL TEST

The mechanical behavior under compressive forces was studied through the compressive strength at fracture. It is defined as the maximum stress carried by the specimen during the test "the peak of the stress-strain curve" [15]. The compressive stress-strain diagrams for the fumarate resin crosslinked with MMA,

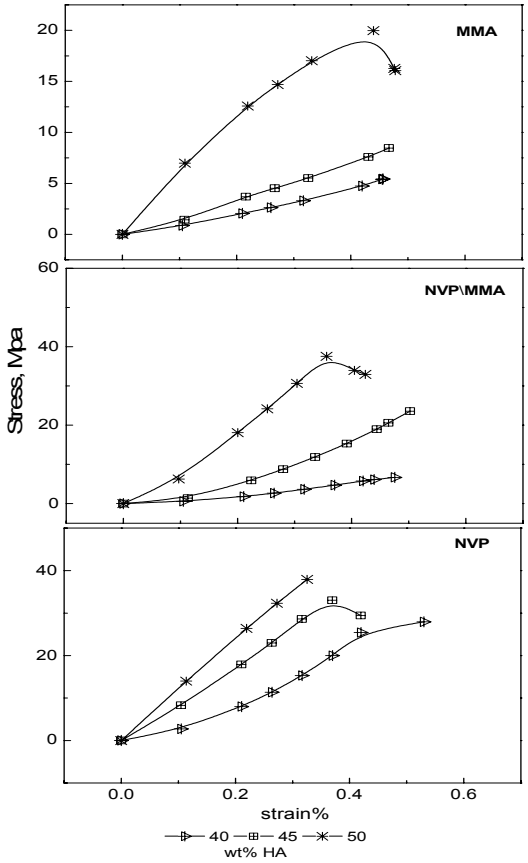

Fig. 15. Compressive strength values of PPF crosslinked with MMA, NVP and NVP/MMA, loaded with different percentage of HA (40, 45 and 50 wt %) before immersion in SBF.

NVP, NVP/MMA loaded with different concentrations of HA (40, 45 and 50 wt%) are given in Figure 15. From the figure it is seen that the compressive strength was 31.35, 14.03 and 6.17 MPa at strain 0.36% for composite filled with 40wt% HA and crosslinked with NVP, NVP/MMA and MMA respectively. It is noticed that the values increased by increasing the filler content [41]. From Figure16, after the period of immersion, these values become higher and reach 51.79, 31.65 and 17.65 for NVP, NVP/MMA and MMA. Similar behavior was observed for other PPF-based formulations [20, 41].

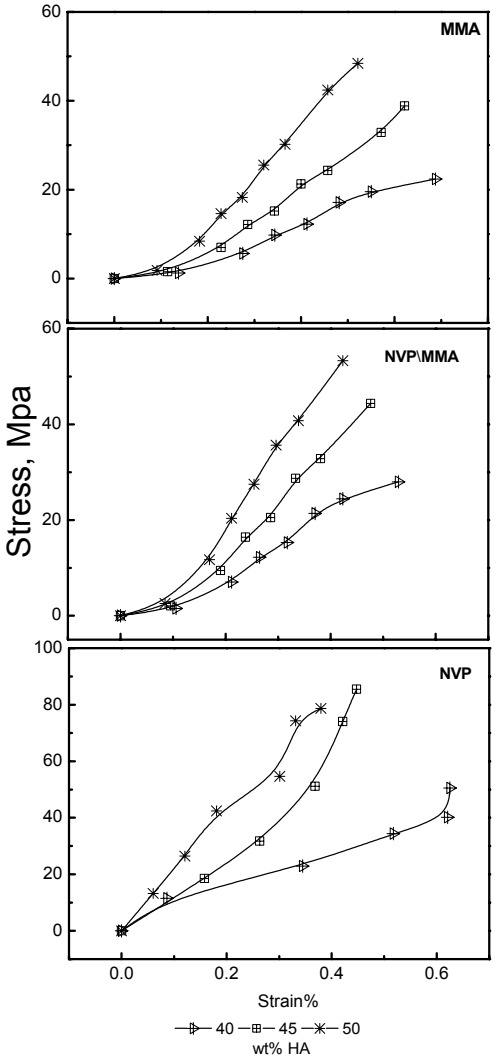

Fig. 16. Compressive strength values of PPF crosslinked with MMA, NVP and, NVP/MMA and loaded with different percentage of HA (40, 45 and 50 wt%) after immersion in SBF.

CONCLUSION

Polypropylene fumarate (PPF) was chosen as unsaturated polyester to be crosslinked with NVP, MMA and NVP/MMA and filled with 40, 45 and 50 wt% hydroxyapatite to be used as bone cement. The formation of bone apatite on the surface of the composites after immersion in simulated body fluid (SBF) was achieved through the change in the intensities of the bands noticed on FTIR charts at wave numbers 1030, 566 cm^{-1} for phosphate group which were found to increase after immersion in SBF.

The bioactivity of the composites was also investigated through the formation of white sphere crystals appeared on the SEM images and phosphocalcic ratios which were found to be very close to the stoichiometric biological apatite (1.67).

The dielectric method was also used to investigate the formation of apatite on the surfaces of composites. The dielectric loss was measured at frequency range 10^2–10^5 Hz and the data obtained were analyzed through Fröhlich and Havriliak-Negami functions. The pronounced increase in relaxation time noticed after immersion in the SBF confirms the bioactivity and gives an evidence to use the method in such purpose.

The addition of nanosized needle-like HA can increase the mechanical properties, decrease the biodegradation rate. The results demonstrate the capability to alter the degradation rate and the mechanical properties of the crosslinked PPF/HA networks so that it can be tailored for specific orthopedic applications.

REFERENCES

1. ABD-EL-MESSIEH, S.L., Dielectric relaxation of binary systems of some disubstituted fumarates with acrylonitrile and vinylacetate in CCl_4 solutions, *J. Mol. Liq*., 2002, **95**, 167–182.
2. ABD-EL-MESSIEH, S.L., K.N. ABD-EL-NOUR, Effect of curing time and sulfur content on the dielectric relaxation of styrene butadiene rubber, *J. Appl. Polym. Sci*., 2003, **88**, 1613–1621.
3. BEN AMOR, I., H. REKIK, H. KADDAMI, M. RAIHANE, M. AROUS, A. KALLEL, Studies of dielectric relaxation in natural fiber-polymer composites, *Journal of Electrostatics*, 2009, **67**, 717–722.
4. CAMPBELL, J.A., A.A. GOODWIN, G.P. SIMON, Dielectric relaxation studies of miscible polycarbonate/polyester blends, *Polymer*, 2001, **42**, 4731–4741.
5. CHEN, F., Z.-C. WANG, C.-J. LIN, Preparation and characterization of nano-sized hydroxyapatite particles and hydroxyapatite/chitosan nano-composite for use in biomedical materials, *Materials Letters*, 2002, **57**, 858–861.
6. CHŁOPEK, J., A. MORAWSKA-CHOCHÓŁ, B. SZARANIEC, The influence of the environment on the degradation of polylactides and their composites, *Journal of Achievements in Materials and Manufacturing Engineering*, 2010, **43**, 72–79.
7. EDUARDO, R-H., K. ARIGA, Y. LVOV, *Bio-inorganic hybrid nanomaterials: strategies, syntheses, characterization and applications*, Publisher Wiley-VCH, Weihneim, 2008.

8. ESLAMI, H., M. SOLATI-HASHJIN, M. TAHRIRI, Synthesis and characterization of hydroxyapatite nanocrystals via chemical precipitation technique, *Iranian Journal of Pharmaceutical Sciences*, 2008, **4**, 127–134.
9. FATHI, M.H., A. HANIFI, V. MORTAZAVI, Preparation and bioactivity evaluation of bone-like hydroxyapatite nanopowder, *Journal of Materials Processing Technology*, 2008, **202**, 536–542.
10. GREGORY, B.K., G. VILLASEÑOR, C.A. DIENER, M. BAUGH, K. MCCOLOUGH, S. MIKACH, A. SCOLA, J. WHITESELL, K. WATSON, Synthesis and characterization of fumarate copolyesters for use in bioresorbable bone cement compositions, *Macromolecular Science, Part A: Pure and Applied Chemistry*, 2006, 43, 855–863..
11. HAOYING, L., Y. CHEN, Y. XIE, Photo-crosslink polymerization to prepare polyanhydrides needle-like hydroxyapatite biodegradable nanocomposites for orthopedic application, *Material Letters*, 2003, **57**, 2848–2854.
12. HAROUN, A.A., V. MIGONNEY, Synthesis and in vitro evaluation of gelatin/hydroxyapatite graft copolymers to form bionanocomposites, *International Journal of Biological Macromolecules*, 2010, **46**, 310–316.
13. HASIRCI, V., K. LEWANDROWSKI, J.D. GRESSER, D.L. WISE, D.J. TRANTOLO, Versatility of biodegradable biopolymers: degradability and an *in vivo* application, *Journal of Biotechnology*, 2001, **86**, 135–150.
14. HAVRILIAK, S., S.J. HAVRILIAK**,** *Dielectric and Mechanical Relaxation in Materials*, Hanser Publishers, Cincinnati, 1997.
15. HE, S., M.D. TIMMER, M.J. YASZEMSKI, A.W. YASKO, P.S. ENGEL**,** A.G. MIKOS, Synthesis of biodegradable poly(propylene fumarate) networks with poly(propylene fumarate)-diacrylate macromers as crosslinking agents and characterization of their degradation products, *Polymer*, 2001, **42**, 1251–1260.
16. HENRY, F., L.C. COSTA, M. DEVASSINE, The evolution of poly(lactic acid) degradability by dielectric spectroscopy measurements, *European Polymer Journal*, 2005, **41**, 2122–2126.
17. HILL, N.E., W.E. VAUGHAN, A.H. PRICE, M. DAVIES, *Dielectric properties and molecular behavior*, Van Nostrand, London, 1969.
18. HU, Y., H.R. MOTZER, A.M. ETXEBERRIA, M.J. FERNANDEZ-BERRIDI, J.J. IRUIN, P.C. PAINTER, M.M. COLEMAN, Concerning the self-association of N-vinyl pyrrolidone and its effect on the determination of equilibrium constants and the thermodynamics of mixing, *Macromol. Chem. Phys*., 2000, **201**, 705–714.
19. JAYABALAN, M., K.T. SHALUMON, M.K. MITHA, K. GANESAN, M. EPPLE, Effect of hydroxyapatite on the biodegradation and biomechanical stability of polyester nanocomposites for orthopaedic applications, *Acta Biomaterial,* 2010, **6**, 3763–775.
20. KAMEL, N.A., T.H. ABOU-AIAAD, B.A. ISKANDER, S.K.H. KHALIL, S.H. MANSOUR, S.L. ABD-EL-MESSIEH, K.N. ABD-EL-NOUR,. Biophysical studies on bone cement composites based on polyester fumarate, *J. Appl. Polym. Sci*., 2010, **116**, 876–885.
21. KARABANOVA, L.V., G. BOITEUX, O. GAIN, G. SEYTRE, L.M. SERGEEVA, E.D. LUTSYK, P.A. BONDARENKO, Semi interpenetrating polymer networks based on polyurethane and polyvinylpyrrolidone. II. Dielectric relaxation and thermal behavior, *J. Appl. Polym. Sci*., 2003, **90**, 1191–1201.
22. KEE-WON, L., S. WANG, M. MICHAEL, J. YASZEMSKI, L. LU, Physical properties and cellular responses to crosslinkable poly(propylene fumarate)/hydroxyapatite nanocomposites, *Biomaterials*, 2008, **29**, 2839–2848.
23. KOKUBO, T., H. KUSHITANI, S. SAKKA, T. KITSUGI, T. YAMAMURO, Solutions able to reproduce *in vivo* surface-structure changes in bioactive glassceramics A-W3, *J. Biomed. Mater. Res*., 1990, **24**, 721–734.

24. KOKUBO, T., Bioactivity of glasses and glass ceramics. In: P. DUCHEYNE, T. KOKUBO, C.A. van BLITTERSWIJK, eds., *Bone-Bonding Materials*, Leiderdorp, The Netherlands, Reed Healthcare Communications, 1992, pp. 31–46.
25. KOLYBABA, M., L.G. TABIL, S. PANIGRAHI, W.J. CRERAR, T., POWELL, B. WANG, Biodegradable polymers: Past, present, and future, *CSAE/ASAE Annual Intersectional Meeting* Sponsored by the Red River Section of ASAE Quality In& Suites 301 3rd Avenue North Fargo, North Dakota, USA October 3–4, 2003.
26. LIU, Q., *Hydroxyapatite/polymer composites for bone replacement*, Ph.D Thesis, Bilthoven, The Netherlands, 1997.
27. MARTINEZ-VALENCIA, A. B., G. CARBAJAL-DE LA TORRE, A. DUARTE MOLLER, H.E. ESPARZA-PONCE, M.A. ESPINOSA-MEDINA, Study of bioactivity, biodegradability and mechanical properties of polyurethane/nano-hydroxyapatite hybrid composites, *International Journal of the Physical Sciences*, 2011, **6**, 6681–6669.
28. McMORROW, B., R. CHARTOFF, D. KLOSTERMAN, Processing and characterization of a carbon nanofiber/vinyl-ester resin composite, *SAMPE 2003 Proceedings*, Long Beach, California, May, 2003.
29. MERRETTK, K., R.M. CORNELIUS, W.G. MCCLUNG, L.D. UNSWORTH, H. SHEARDOWN, Surface analysis methods for characterizing polymeric biomaterials, *J. Biomater. Sci. Polym. Ed.*, 2002, **13**, 593–621.
30. MICULESCU, F., L.T. CIOCAN, M. MICULESCU, A. ERNUTEANU, Effect of heating process on microstructure level of cortical bone prepared for compositional analysis, *Digest Journal of Nanomaterials and Biostructures*, 2011, **6**, 225–233.
31. MOHAMED, M.G., S.L. ABD-EL-MESSIEH, S. EL-SABBAGH, A.F. YOUNAN, Electrical and mechanical properties of polyethylene-rubber blends, *J. Appl. Polym. Sci.,* 1998, **69**, 775–783.
32. MOON, G., S.S. IM, Dielectric spectroscopy of conductive polyaniline salt films, *J. Appl. Polym. Sci*., 2001, **82**, 2760–2769.
33. MORENO, S., R.G. RUBIO, G. LUENGO, F. ORTEGA, M.G. PROLONGO, Dielectric relaxation of poly (ethylenglycol)-b-poly (propylenglycol)-b-poly(ethylenglycol) copolymers above the glass transition temperature, *Eur. Phys. J. E*., 2001, **4**, 173–182.
34. NAIR, L.S., C. T. LAURENCIN**,** Polymers as biomaterials for tissue engineering and controlled drug delivery, *Adv. Biochem. Engin\Biotechnol*., 2006, **102**, 47–90.
35. NASSER, A.M., T. BARAKA, M.S. KHIL, A.M. OMRAN, F.A. SHEIKH, H.Y. KIM, Extraction of pure natural hydroxyapatite from the bovine bones biowaste by three different methods, *Journal of Materials Processing Technology,* 2009, **209**, 3408–3415.
36. PISSIS, P., A. KYRITSIS, A.A. KONSTA, D. DAOUKAKI, Polymer-water interactions in PAA hydrogels, *Colloids Surf. A*, 1999, **149**, 253–262.
37. RAMESH, S., A.H. YAHAYA, A.K. AROF, Dielectric behavior of PVC based polymer electrolytes, *Solid State Ionics*, 2001, **152–153**, 291–294.
38. REDDY, C.V.S., X. HAN, Q.-Y. ZHU, L.-Q. MAI, W. CHEN, Dielectric spectroscopy studies on (PVP and PVA) polyblend film, *Microelectronic Engineering*, 2006, **83**, 281– 285.
39. SENGWA, R.J., S. SANKHLA, Dielectric dispersion study of coexisting phases of aqueous polymeric solution: Poly (vinyl alcohol) + poly (vinyl pyrrolidone) two-phase systems, *Polymer*, 2007, **48**, 2737–2744.
40. SHARMA, V.P., V. AGARWAL, S. UMAR, A.K. SINGH, Polymer composites sustainability: environmental perspective, future trends and minimization of health risk, *2nd International Conference on Environmental Science and Development*, 2011, IPCBEE 4, IACSIT Press, Singapore, 2011.
41. TIMMER, M.D., C.G. AMBROSE, A.G. MIKOS, In vitro degradation of polymeric networks of poly(propylene fumarate) and the crosslinking macromer poly(propylene fumarate)-diacrylate, *Biomaterials*, 2003, **24**, 571–577.

42. TSONOS, C., L. APEKIS, K. VIRAS, L. STEPANENKO, L. KARABANOVA, L.M. SERGEEVA, Electric and dielectric behavior in blends of polyurethane-based ionomers, *Solid State Ionics*, 2001, **143**, 229–249.
43. YAN, J., J. LI, M.B. RUNGE, M. DADSETAN, Q. CHEN, L. LU, M.J. YASZEMSKI, Crosslinking characteristics and mechanical properties of an injectable biomaterial composed of polypropylene fumarate and polycaprolactone copolymer, *J. Biomater. Sci. Polym. Ed*., 2011, **22**, 489–504.